Limit on the Detectability of the Energy Scale of Inflation

Lloyd Knox and Yong-Seon Song
Department of Physics, One Shields Avenue, University of California, Davis, California 95616
(Received 18 February 2002; published 18 June 2002)

We show that the polarization of the cosmic microwave background can be used to detect gravity waves from inflation if the energy scale of inflation is above 2×10^{15} GeV. These gravity waves generate polarization patterns with a curl, whereas (to first order in perturbation theory) density perturbations do not. The limiting "noise" arises from the second-order generation of curl from density perturbations, or rather residuals from its subtraction. We calculate optimal sky coverage and detectability limits as a function of detector sensitivity and observing time.

DOI: 10.1103/PhysRevLett.89.011303 PACS numbers: 98.70.Vc, 98.65.Dx, 98.80.Cq

Few ideas have had greater impact in cosmology than that of inflation [1–3]. The simplest models of inflation make four predictions, three of which provide very good descriptions of data: the mean curvature of space is vanishingly close to zero, the power spectrum of initial density perturbations is nearly scale invariant, and the perturbations follow a Gaussian distribution. As the data have improved substantially (e.g., [4–6]) they have agreed well with inflation, whereas all competing models for explaining the large-scale structure in the Universe have been ruled out (e.g., [7–9]).

We must note though that these three predictions are all fairly generic [10]. Further, although existing models for the formation of structure have been ruled out, there is no proof of inflation's unique ability to lead to our Universe. Indeed, alternatives are being invented [11].

The fourth (and yet untested) prediction may therefore play a crucial role in distinguishing inflation from other possible early Universe scenarios. Inflation inevitably leads to a nearly scale-invariant spectrum of gravitational waves, which are tensor perturbations to the spatial metric. Detection of these gravity waves might allow discrimination between competing scenarios (e.g., [11]) and different inflationary models (e.g., [12]).

The amplitude of the power spectrum of tensor perturbations to the metric is directly proportional to the energy scale of inflation. One can use a determination of the tensor contribution to cosmic microwave background (CMB) temperature anisotropy, here parametrized by the quadruple variance, to determine this energy scale [13]:

$$V_*^{1/4}/m_{Pl} = 1.15\langle Q_T^2\rangle^{1/4} = 3.0 \times 10^{-3} r^{1/4}, \quad (1)$$

where $r \equiv \langle Q_T^2\rangle/\langle Q_S^2\rangle$, S stands for scalar (density) perturbation, and $\langle Q_S^2\rangle \simeq 4.6 \times 10^{-11}$ from observations [14]. Currently the energy scale of inflation remains uncertain by at least 12 orders of magnitude. Its determination could be crucial to understanding how inflation arises in a fundamental theory of physics.

In Fig. 1 we show the angular power spectrum of CMB temperature perturbations contributed by scalar perturbations and by tensor perturbations with $r = 10^{-3}$. By determining the total CMB temperature power spectrum we can determine or limit the energy scale of inflation, based on the presence or absence of extra power at low l. The scalar temperature perturbations inevitably limit our ability to detect the tensor temperature perturbations to those cases with $r > r_{\rm lim} = 0.13$ [15,16].

In [17,18] it was pointed out that tensor perturbations result in CMB polarization patterns with a curl, whereas scalar perturbations do not. By analogy with electromagnetism, these modes are called "B modes," and the curl-free modes are called "E modes." This was an exciting

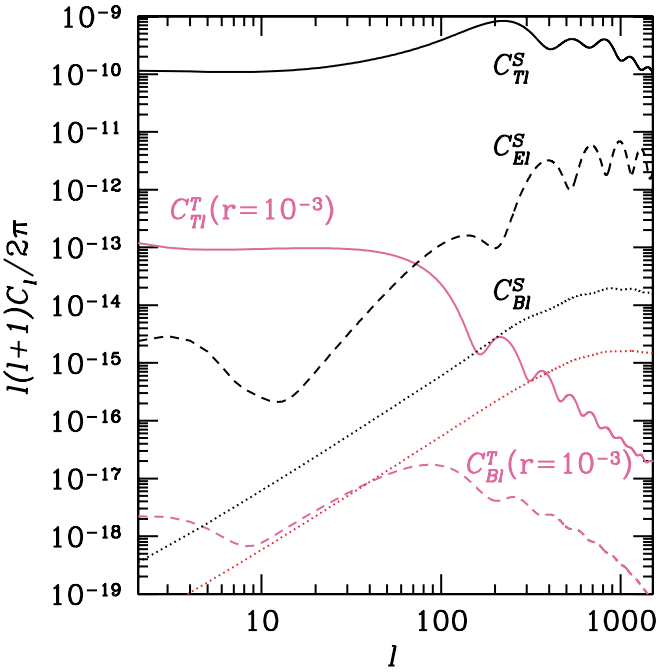

FIG. 1 (color online). Angular power spectra. The solid lines are for temperature anisotropies due to scalar perturbations, C_{Tl}^S and tensor perturbations C_{Tl}^T with $r = 10^{-3}$. The dashed lines are for the E modes from scalar perturbations C_{El}^S and the B modes from tensor perturbations C_{Bl}^T. The dotted lines are for the lensing-induced scalar B modes C_{Bl}^S before (above) and after (below) the cleaning that can be done by a perfect experiment. The feature at $\ell < 10$ is due to reionization which we assume occurs at $z_{\rm ri} = 7$.

development, because the new signature of tensor perturbations could not be confused with scalar perturbations. Figure 1 also shows the power spectrum of this B mode with the amplitude it would have if $V_*^{1/4} = 6.4 \times 10^{15}$ GeV, corresponding to $r = 10^{-3}$. It is a very weak signal, even at its peak it is $\sim 10^7$ times less than the power spectrum of the temperature anisotropy. Ignoring any contaminating source of curl-mode polarization, the detectability limit is solely a matter of sufficient sensitivity to the CMB polarization. For a detector of sensitivity s uniformly observing the entire sky for time t,

$$r_{\rm lim} = 10^{-2}\left(\frac{s}{\mu{\rm K\,sec}^{1/2}}\right)^2\left(\frac{t}{1\ {\rm yr}}\right)^{-1}. \tag{2}$$

Equation (2) [19] does not take into account a contaminating source of B mode that arises from the lensing of the E mode by density perturbations along lines of sight between the observer and the last-scattering surface [20]. This scalar contribution to the B-mode power spectrum is shown in Fig. 1. As we will see below this contamination sets the detectability limit at $r_{\rm lim} = 2.6 \times 10^{-4}$, similar to what was found in [21].

This lensing contaminant can be cleaned from the maps as discussed in [22,23]. Here we show that there are limits to how well this can be done. Our main result is that tensor perturbations can be detected only if $V_*^{1/4} > 2 \times 10^{15}$ GeV. Interestingly, this is below the energy scale for the gauge coupling-constant convergence at 10^{16} GeV in minimal extensions to the standard model of particle physics (e.g., [24]).

The Stokes parameters, I, Q, and U are related to the unlensed Stokes parameters (denoted with a tilde) by

$$\begin{aligned} I(\vec{\theta}) &= \tilde{I}(\vec{\theta} + \delta\vec{\theta})Q(\vec{\theta}) = \tilde{Q}(\vec{\theta} + \delta\vec{\theta})U(\vec{\theta}) \\ &= \tilde{U}(\vec{\theta} + \delta\vec{\theta})\,. \end{aligned} \tag{3}$$

The deflection angle, $\delta\vec{\theta}$, is the tangential gradient of the projected gravitational potential,

$$\phi(\vec{\theta}) = 2\int dr\,\frac{(r - r_s)}{r r_s}\,\Psi(r\hat{n}, r)\,, \tag{4}$$

where r is the coordinate distance along our past light cone, s denotes the CMB last-scattering surface, and $\hat{n}$ is the unit vector in the $\vec{\theta}$ direction. The effect on the B mode power spectrum is [20]

$$C_{Bl} = C_{\tilde{B}l} + \sum_{l'} W_l^{l'} C_{\tilde{E}l'}\,, \tag{5}$$

where

$$W_l^{l'} = \frac{l'^3}{4}\int_0^\pi \theta\,d\theta\left\{\sigma_2^2(\theta)\left[J_0(l\theta)J_2(l'\theta) - \frac{1}{2}J_4(l\theta)[J_2(l'\theta) + J_6(l'\theta)]\right] + \sigma_0^2(\theta)[J_4(l\theta)J_4(l'\theta) + J_0(l'\theta)J_0(l\theta)]\right\}. \tag{6}$$

The functions $\sigma_2^2(\theta)$ and $\sigma_0^2(\theta)$ depend on the statistical properties of the displacement potential ϕ and are given by

$$\begin{aligned} \sigma_0^2(\theta) &= \int \frac{l\,dl}{2\pi}\,l^2 C_l^\phi[1 - J_0(l\theta)], \\ \sigma_2^2(\theta) &= \int \frac{l\,dl}{2\pi}\,l^2 C_l^\phi J_2(l\theta)\,, \end{aligned} \tag{7}$$

where

$$C_l^\phi \equiv \langle \phi_{lm}\phi_{lm}^*\rangle \tag{8}$$

and ϕ_{lm} is the spherical-harmonic transform of $\phi(\vec{\theta})$.

If we have a means of determining ϕ, and therefore $\delta\vec{\theta}$, we can reconstruct the unlensed maps from the lensed maps by use of Eq. (3). This procedure cleans out the lensing-induced B mode. The C_l^ϕ above can either be interpreted as the power spectrum of the lensing potential (in the case of uncleaned maps, in which case we will call it $C_l^{\phi(S)}$) or the power spectrum of the lensing potential residuals (in the case of lensing-cleaned maps). In the uncleaned case [25] (in the Limber approximation valid at small scales):

$$C_l^{\phi(S)} = \frac{8\pi^2}{l^3}H_0^2\int_0^{r_s} dr\,r\left[\frac{(r - r_s)}{r r_s}\right]^2 \Delta_\Phi^2(k, r)\Big|_{k=l/r}\,, \tag{9}$$

where r_s is the comoving distance to the last-scattering surface and $\Delta_\Phi^2(k, r) \equiv k^3/(2\pi)^2 P_\Phi(k, r)$, where $P_\Phi(k, r)$ is the power spectrum of the gravitational potential at the time corresponding to coordinate distance r on our past light cone. We plot $C_l^{\phi(S)}$ in Fig. 2

We consider the ϕ reconstruction procedure given in [23] which exploits the fact that lensing leads to a mode-mode coupling with expectation value proportional to ϕ. Their estimator is a minimum-variance (MV) average over pairs of map modes with $l \neq l'$. Since we know the statistics of the signal, C_l^ϕ, we can Wiener filter (WF) the MV estimate and further reduce the errors in the reconstruction. The error in the WF estimate of ϕ_{lm} has variance:

$$C_l^{\phi({\rm WF})} = \frac{C_l^{\phi(S)} C_l^{\phi({\rm MV})}}{C_l^{\phi(S)} + C_l^{\phi({\rm MV})}}\,. \tag{10}$$

The Wiener-filtering is important for $l \gtrsim 500$, where $C_l^{\phi(S)}/C_l^{\phi({\rm MV})} < 1$. Note that we assume negligible uncertainty in the underlying cosmological model, which we expect to be valid by the time B modes are detected.

Cleaning can greatly reduce the amplitude of C_l^ϕ, as shown in Fig. 2 where the angular power spectrum of the residual ϕ is shown for two different experiments. The first is the "reference" experiment of [23] which makes temperature maps with weight-per-solid angle of $w = (1\ \mu{\rm K\,arcmin})^{-2}$ and Q and U maps each with half this weight, all with $7'$ (full width at half maximum) resolution.

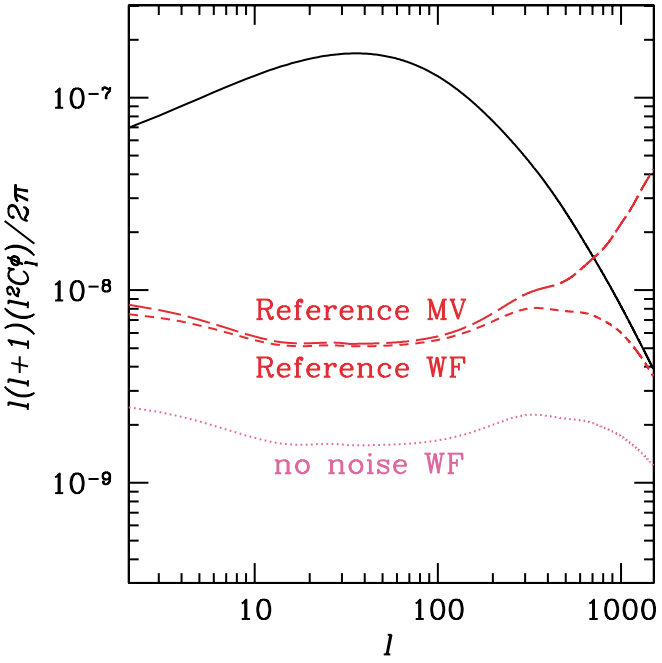

FIG. 2 (color online). Angular power spectrum of projected gravitational potential ϕ (solid curve) and the power spectrum of the residuals of different reconstruction procedures: minimum variance for the reference experiment (long dashed line), Wiener filter for the reference experiment (short dashed line), and Wiener filter for a noiseless experiment (dotted line).

As can be seen in Fig. 2 a no-noise, perfect angular resolution experiment still results in nonzero ϕ residuals. Although the number of modes at multipole moment ℓ rises like ℓ, the signal-to-noise ratio for ϕ reconstruction from each pair of modes is dropping more rapidly. The level of mode-mode coupling (the signal for lensing reconstruction) is proportional to the unlensed power spectra which drop exponentially. The mode-mode coupling noise is the sample variance of the *lensed* power spectra and these drop less rapidly. Higher-order correlations could conceivably be used for improved ϕ reconstruction. Significant improvement is improbable though since these estimators will likely also have noise (signal) scaling with lensed (unlensed) power spectra.

Because the cleaning is not perfect, there is still lensing-induced scalar B mode in the cleaned maps. In the no-noise limit the residual scalar B-mode power spectrum, $C_{Bl}^{\rm WF}$, has been reduced by a factor of 10 from the uncleaned amplitude, as shown in Fig. 1.

All of the above results are for $f_{\rm sky} = 1$. Given a detector (or array of detectors) with total sensitivity s and an amount of observing time t there is an optimal amount of sky to cover given by $f_{\rm sky}^{\rm opt} = 10^{-8}\ (\mu{\rm K})^2 t/s^2$. In Fig. 3 we plot $r_{\rm lim}$ as a function of s^2/t assuming optimal sky coverage (constrained to $f_{\rm sky} \leq 1$). The detectability limit is not strongly sensitive to deviations from optimal sky coverage, which is fortunate since other considerations can influence sky coverage choice as well. Note that $s^2/t = 10^{-8}\ (\mu{\rm K})^2$ could be achieved by observing for a year with an array of 30 000 detectors each with sensitivity 100 $\mu{\rm K\,sec}^{1/2}$. We have ignored aliasing of the scalar E mode which can be important for $f_{\rm sky} \neq 1$, as studied in [21]. Aliasing considerations increase $f_{\rm sky}^{\rm opt}$ and $r_{\rm lim}$. For $s^2/t = 10^{-7}\ (\mu{\rm K})^2$ and $f_{\rm sky} = 1$, $r_{\rm lim} = 3 \times 10^{-4}$. Therefore, aliasing effects will not increase $r_{\rm lim}$ by more than 40% over our results, as shown in Fig. 3.

Increasing reionization redshift decreases the detectability limit, due to the extra low ℓ power (see Fig. 1). For $z_{\rm ri} = 10$, $r_{\rm lim} = 1.4 \times 10^{-5}$ in the $s^2/t = 0$ limit. Figure 3 also shows results for no reionization, which is roughly equivalent to ignoring modes with $l \lesssim 10$.

The projected gravitational potential out to some limiting redshift, $z_{\rm lim}$, can, in principle, be reconstructed from peculiar velocity measurements [26] or analysis of the statistical distribution of apparent galaxy shapes. Subtracting the lensing contaminant, calculated from this reconstruction, from CMB maps leaves only the contribution from $z > z_{\rm lim}$. The effect of this remaining lensing can be calculated by altering the lower limit of integration in Eq. (9)from 0 to $r(z_{\rm lim})$. To improve upon the noise-free self-cleaned maps result of $r_{\rm lim} = 2.4 \times 10^{-5}$, one needs to take $z_{\rm lim} \gtrsim 7$.

Our analysis ignores polarized emission from galactic and extragalactic sources. Multifrequency observations can be used to clean out these signals based on their distinct spectral shapes. However, even in the no-noise limit these cannot be cleaned perfectly since their spectral shapes are not perfectly well known and vary spatially (e.g., [27]). Our estimate of the detectability limit should be viewed as a lower limit.

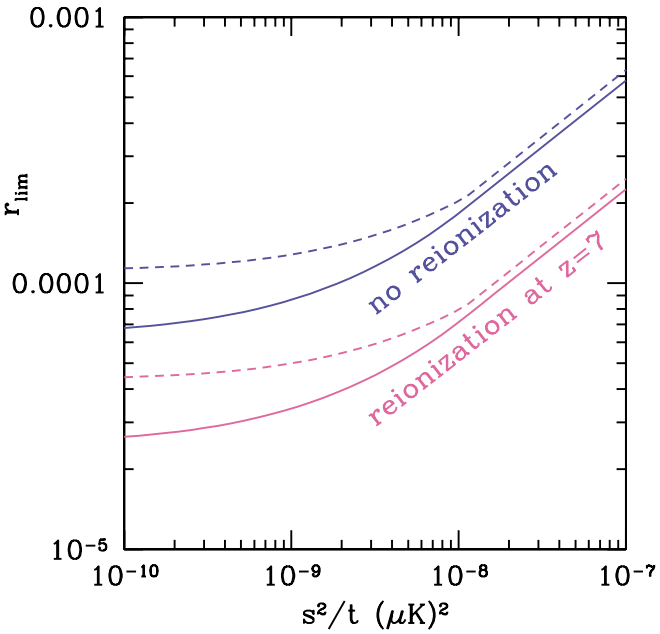

FIG. 3 (color online). Achievable detectability limit as a function of total detector array sensitivity s and observing time t, assuming optimal sky coverage (solid curves) and one-third of optimal sky coverage (dashed curves).

How likely is it that the energy scale of inflation is high enough to be determined? It is conceivable that $V_*^{1/4}$ is as low as 10^3 GeV [28]. Given even odds between 10^3 and 10^{19} GeV the chances are small. On the other hand, gauge coupling unification gives us a hint that something interesting may be occurring at 10^{16} GeV. If inflation has anything to do with grand unification, or physics at higher energy scales, then the chances are good.

The likelihood of detection may also be addressed by better determination of the scalar spectrum. If we assume particular functional forms for $V(\phi)$ and a scalar perturbation spectrum with power-spectral index n, near the scale-invariant value of unity, then we can give constraints on the range of possible values of r. Here we follow the nomenclature and calculations of [12]. Exponential potentials have $r = 5(1 - n)$ and "small-field polynomial" potentials $\{V(\phi) = \Lambda^4[1 - (\phi/\mu)^p]\}$ with $p = 2$ having $r = 10\exp[-50(1 - n)]$. Still other classes of models (hybrid inflation and the small-field polynomial potentials with $p > 2$) leave little or no relationship between r and n; r can take on detectable values or vanishingly small ones. Perhaps the happiest case is the simplest one: polynomial potentials with $V(\phi) = \Lambda^4(\phi/\mu)^p$. With $p \geq 2$ all have $r > 0.1$, well above our detectability limit.

In summary, we have calculated how large the amplitude of tensor perturbations must be in order for their effect on the CMB to be distinguishable from those of lensing. By reconstructing the lensing potential, using the mode-mode coupling induced by lensing, one can reduce the lensing contamination but not eliminate it. The residual lensing signal prevents detection of tensor perturbations if $V_* < (2 \times 10^{15}\ \text{GeV})^4$. If V_* is slightly larger, then an ambitious observational program may succeed in determining the energy scale of inflation—possibly a key step towards finding inflation a comfortable home in a fundamental theory of physics.

We thank A. Albrecht, D. Chung, N. Dalal, and J. Kiskis for useful conversations. We used the program CMBFAST for some of our calculations [29].

[1] A. H. Guth, Phys. Rev. D **23**, 347 (1981).
[2] A. Albrecht and P. J. Steinhardt, Phys. Rev. Lett. **48**, 1220 (1982).
[3] A. D. Linde, Phys. Lett. **114B**, 431 (1982).
[4] C. B. Netterfield *et al.,* astro-ph/0104460.
[5] A. T. Lee *et al.,* Astrophys. J. Lett. **561**, L1 (2001).
[6] N. W. Halverson *et al.,* astro-ph/0104489.
[7] U. Pen, U. Seljak, and N. Turok, Phys. Rev. Lett. **79**, 1611 (1997).
[8] B. Allen *et al.,* Phys. Rev. Lett. **79**, 2624 (1997).
[9] A. Albrecht, R. A. Battye, and J. Robinson, Phys. Rev. Lett. **79**, 4736 (1997).
[10] For example, a much more impressive success would be the prediction of *features* in the power spectrum followed by their detection.
[11] J. Khoury, B. A. Ovrut, P. J. Steinhardt, and N. Turok, Phys. Rev. D **64**, 123522 (2001).
[12] S. Dodelson, W. H. Kinney, and E. W. Kolb, Phys. Rev. D **56**, 3207 (1997).
[13] M. S. Turner and M. White, Phys. Rev. D **53**, 6822 (1996).
[14] The * subscript on V means that it is evaluated when the scale factor is about e^{50} times smaller than it is at the end of inflation, when the relevant perturbations for large-scale CMB fluctuations are exiting the horizon. There is a slight dependence on Ω_Λ [30]. We assume throughout that $\Omega_\Lambda = 1 - \Omega_m = h = 0.65$, $\Omega_b = 0.05$, $\delta_H = 4.2 \times 10^{-5}$, and $z_{\rm ri} = 7$.
[15] L. Knox and M. S. Turner, Phys. Rev. Lett. **73**, 3347 (1994).
[16] Here and throughout, the detection limit is set at 3.3 times the standard deviation. For a normal distribution this means that one can make a detection at a 95% confidence level for 95% of possible realizations.
[17] M. Kamionkowski, A. Kosowsky, and A. Stebbins, Phys. Rev. Lett. **78**, 2058 (1997).
[18] U. Seljak and M. Zaldarriaga, Phys. Rev. Lett. **78**, 2054 (1997).
[19] M. Kamionkowski and A. Kosowsky, Phys. Rev. D **57**, 685 (1998).
[20] M. Zaldarriaga and U. Seljak, Phys. Rev. D **58**, 023003 (1998).
[21] A. Lewis, A. Challinor, and N. Turok, astro-ph/0108251.
[22] W. Hu, Phys. Rev. D **65**, 023003 (2002).
[23] W. Hu and T. Okamoto, astro-ph/0111606.
[24] P. Langacker and M. Luo, Phys. Rev. D **44**, 817 (1991).
[25] W. Hu, Phys. Rev. D **62**, 043007 (2000).
[26] E. Bertschinger and A. Dekel, Astrophys. J. Lett. **336**, L5 (1989).
[27] M. Tegmark, D. J. Eisenstein, W. Hu, and A. de Oliveira-Costa, Astrophys. J. **530**, 133 (2000).
[28] L. Knox and M. S. Turner, Phys. Rev. Lett. **70**, 371 (1993).
[29] U. Seljak and M. Zaldarriaga, Astrophys. J. **469**, 437 (1996).
[30] L. Knox, Phys. Rev. D **52**, 4307 (1995).